2018 European Control Conference (ECC)
June 12-15, 2018. Limassol, Cyprus

A Novel Design of Maximum Power Point/Droop Controllers for Photovoltaic Sources in DC Microgrids

Konstantinos F. Krommydas, *Member, IEEE* and Antonio T. Alexandridis, *Member, IEEE*

***Abstract*— In this paper, we consider the challenging problem of operating photovoltaic (PV) sources in direct current (dc) microgrids at maximum power point (MPP) under normal conditions and in droop control operation when a sudden disconnection from the main grid occurs. Based on some recently proposed control design results, we present an augmented cascaded control scheme with improved stability properties that fulfills the following: 1) drives the PV sources energy production at MPP when the dc microgrid is connected to the main grid, 2) achieves accurate power sharing among the PV sources when the dc microgrid is disconnected from the main grid, 3) needs no communication between the PV sources, 4) automatically implements the transition between the MPP and the power sharing mode in a smooth, autonomous and seamless manner. In order to prove that the aforementioned aims are satisfied, a rigorous stability analysis is carried out on the accurate dynamic closed-loop system. Furthermore, a tuning method is proposed for the complete control scheme in order to achieve the desired dynamical responses under the time scale separation principle between the cascaded control-loops. Finally, the excellent performance of the control strategy is validated through simulation results and in comparison with the conventional switching mode controller response.**

I. Introduction

Direct current (dc) microgrids are becoming popular due to their ability to easily integrate modern loads, renewable energy sources (RES), and energy storage systems since most of them (i.e. photovoltaic (PV) sources, batteries, electric vehicles) are naturally dc [1]. In addition, dc microgrids do not face problems such as reactive power compensation, frequency stability and synchronization which make them more and more popular in power systems [2].

In this field, the existing control strategies can be divided into two main categories: centralized [3], [4] and decentralized ones [5], [6], [7]. In the first approach, a central controller communicates with all the distributed generation (DG) units using communication links. The drawback of this approach is the need for a communication infrastructure. Moreover, communication systems, especially in large systems, might not be economical or practical, while due to the communication links delay or failure, the reliability of the system may deteriorate. In the second approach, the controller of the DG units needs only local measurements. Due to its modularity and reliability, these methods have been more popular in dc microgrids.

K. F. Krommydas is with the Department of Electrical and Computer Engineering, University of Patras, Rion 26504, Greece. krommydas@ece.upatras.gr

A. T. Alexandridis is with the Department of Electrical and Computer Engineering, University of Patras, Rion 26504, Greece. a.t.alexandridis@ece.upatras.gr

Furthermore, in [8], a comparative stability analysis for current mode and voltage mode droop controllers in dc microgrids is presented. In [9], an active damping method to overcome instability problems of dc microgrids has been proposed, while in [10], a robust controller is developed based on semidefinite programming in order to guarantee and expand the stability region using energy storage. In [11], a distributed control method is proposed to simultaneously optimize the power sharing among sources of islanded dc microgrids, while regulating the distribution bus voltage. In [12], the stability of a dc microgrid is analyzed in modular form wherein only the current inner-loop controllers are considered. A distributed optimal control of dc microgrids is also reported in [13] where the optimal power flow problem is formulated as an exact second order cone program. However, in all the aforementioned cases the accurate dynamics of the RES were not taking into account, but instead they were considered as voltage or current sources. However, as reported in [14], this modeling simplification in the control design and stability analysis may have a negative impact on the actual dc microgrid performance.

In view of these results, the integration of the accurate RES dynamics into the dc microgrid control design seems to be essential. Among the RES, the use of PV has grown exponentially, since they can be installed in every location and require little maintenance effort. Therefore, many researchers have studied PV-based dc microgrids. In [15], a procedure is presented in order to match a maximum power point (MPP) tracking algorithm with the droop controller. Still, only MPP operation is assumed. The study [16] develops a dynamic droop scheme for PV systems to ensure an efficient load sharing operation even when the input renewable power varies. However, it is not examined how this controller will perform when the dc microgrid is connected to the main grid. In [17] and [18], proper controllers are designed to combine MPP with droop control operation. However, in both cases a switching procedure is needed to change from one controller to the other and thus it is not clear how the system will response in this sudden changes.

In [19], an interesting decentralized control strategy for PV sources is presented to unify MPP and droop control operation. With the proposed control scheme, the PV sources will output the maximum available power when they are grid-connected and seamlessly switch to the power sharing mode when it is necessary. Additionally, a steady-state analysis is carried out in order to provide a tuning procedure for the droop control coefficient. However, the lack of any dynamic analysis of the control scheme leaves open questions regard-

ing the performance and robustness of the control design.

In the present paper, taking into account the aforementioned limitations, a unified control scheme is presented, based on [19], with main contributions summarized in:

1) The accurate dynamics of both the PV sources and the power converters are taken into account.
2) A novel augmented cascaded control scheme is proposed with suitable modifications in order to ensure the stability properties of the closed-loop system.
3) A rigorous stability analysis is carried out which achieves to prove that the control objectives in all the cascaded controller levels are fulfilled.
4) A tuning method is presented that determines the controllers gains in order to achieve the desired dynamic response.

The rest of the paper is organized as follows. In Section II, the complete dynamic model of the dc microgrid with the PV sources is provided. In Section III, the control scheme is presented, while in Section IV an extensive stability analysis is carried out. In Section V a tuning method is proposed for the cascaded control system. Simulation results are documented in Section VI, followed by conclusions made in Section VII.

II. System Modeling

The PV source is described by its current-voltage characteristic function, as [20]

$$I_{pv} = n_p I_{ph} - n_p I_{rs}\left[exp\left(\frac{q}{k\vartheta A}\frac{V_{pv}}{n_s}\right) - 1\right] \qquad (1)$$

where n_p is the number of PV modules in parallel, n_s is the number of PV cells in series, I_{rs} is the reverse saturation current of a $p-n$ junction, $q\big(=1.602\times10^{-19}C\big)$ is the unit electric charge, $k\left(=1.38\times10^{-23}J/K\right)$ is Boltzman's constant, ϑ is the $p-n$ junction temperature (in Kelvin), A is the ideality factor, I_{ph} is the short-circuit current of one string of the PV panels and V_{pv} is the PV source voltage. Different curves of a PV source are illustrated in Fig. 1.

A typical dc microgrid configuration with PV sources is shown in Fig. 2. This system consists of a number of PV sources connected to a common dc-bus in parallel with a dc load. Usually dc/dc boost converters are used as the interface unit since they can boost the voltage of the PV sources at a desired voltage level while simultaneously provide a fast and reliable control input. Also, an ac/dc power converter is used to connect the dc microgrid with the main grid when it is desired. For the dynamic analysis of the system power converters, the average modeling technique is adopted [21], which has been extensively used in literature for pulse width modulation regulated systems. Hence, one can obtain the following nonlinear model for the dc microgrid in islanded mode

$$L_i\dot{I}_{pv,i} = -r_i I_{pv,i} - m_{pv,i}V_{dc} + V_{pv,i} \qquad (2)$$

$$C\dot{V}_{dc} = -\frac{V_{dc}}{R} + \sum_{i=1}^{n} m_{pv,i}I_{pv,i} \qquad (3)$$

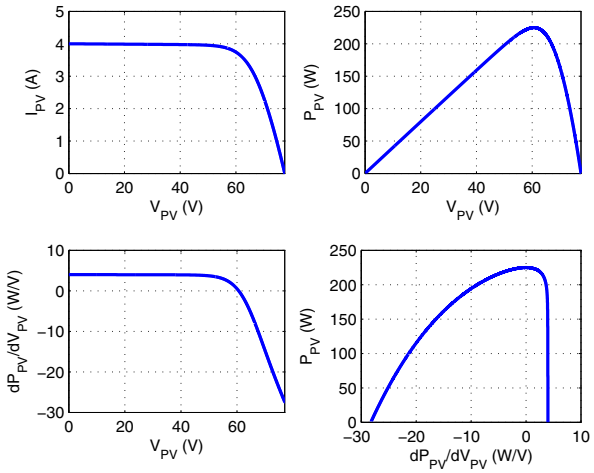

Fig. 1. Different curves of a PV source.

where $I_{pv,i}$ is the PV current injected from the i PV source, V_{dc} is the voltage of the dc-bus, $m_{pv,i}$ represents the duty-ratio of the $i-$boost converter and constitutes the control input, whereas the system parameters are given in detail in Table I. When the system operates in grid-connected mode, the ac/dc power converter drives the dc-bus voltage very fast to its reference value and thus we assume that $V_{dc} = V_{dc,ref}$.

III. Control Design

The aim of the control design is to provide a decentralized control scheme which does not require communication between the control parts of the dc microgrid and can achieve the following objectives:

1) In the grid-connected mode the PV sources should carry out MPP operation, since the power balance of the dc microgrid (i.e. $V_{dc} = V_{dc,ref}$) is maintained from the grid-connected ac/dc converter.
2) When interconnection with the grid is not possible, the PV sources should accurately share the load in proportion to their power ratings and simultaneously regulate the dc-bus voltage at a desired reference.
3) In all cases the system must exhibit a stable performance and converge to the admissible equilibrium point.

In this frame, we present the following three-loop (augmented) cascaded control scheme:

A. Inner-Loop Current-Mode Controller

For the inner-loop, the following controller proposed in [22] is used

$$m_{pv,i} = \frac{1}{V_{dc}}\left(k_{P,i}\left(I_{pv,i} - I_{pv,iref}\right) + k_{I,i}w_i\right) \qquad (4)$$

$$\dot{w}_i = I_{pv,i} - I_{pv,iref} \qquad (5)$$

where $k_{P,i}$, $k_{I,i}$ are positive constants and $I_{pv,iref}$ is the current reference signal. The task of the controller (which is actually a PI controller) is to regulate the current at the reference value $I_{pv,iref}$, which is determined from the middle-loop controller presented in the sequel.

B. dP/dV-Based MPP Modified Controller

For the middle-loop, the following feedback controller is proposed

$$I_{pvref,i} = k_{Pmpp,i}\left(\frac{dP_{pv,i}}{dV_{pv,i}}ref - \frac{dP_{pv,i}}{dV_{pv,i}}\right) + k_{Impp,i}\int\left(\frac{dP_{pv,i}}{dV_{pv,i}}ref - \frac{dP_{pv,i}}{dV_{pv,i}}\right)dt \quad (6)$$

where $k_{Pmpp,i}$, $k_{Impp,i}$ are positive constants and $\frac{dP_{pv,i}}{dV_{pv,i}}ref$ is the reference signal of the power-voltage gradient.

Note that when $\frac{dP_{pv,i}}{dV_{pv,i}}ref = 0$ then (6) operates as MPP tracking controller. For more details about this MPP control strategy the reader can refer to our previous work in [23]. When $\frac{dP_{pv,i}}{dV_{pv,i}}ref \neq 0$, the PV sources leave the MPP operation. The appropriate reference signal $\frac{dP_{pv,i}}{dV_{pv,i}}ref$ is automatically activated when grid disconnection occurs as the following outer-loop controller indicates.

C. Droop Controller

For the outer-loop, the following modified droop controller is proposed

$$\frac{dP_{pv,i}}{dV_{pv,i}}ref = m_i\left(V_{dc,ref}^2 - V_{dc}^2\right) \quad (7)$$

where m_i is a positive constant and $V_{dc,ref}$ is the desired dc-bus voltage value. Apparently, (7) is immediately activated when the regulation of V_{dc} to its reference is lost, i.e. when grid disconnection occurs. Then, the droop characteristics of (7) create the suitable output that achieves accurately power sharing among the PV sources.

It is important to mention at this point that conventional droop controllers use the error signal $(V_{dc,ref} - V_{dc})$. However, using instead the square values of the dc-bus voltage and its reference, leads to substantial improvements both for the calculation of the system's equilibrium point and the stability analysis as it will be shown in the sequel.

Remark 1: It is worth noting that a similar cascaded approach has been presented in [19] which is substantially modified in our work in order to meet stability characteristics. Additionally, with respect to (6), it is demonstrated in [24] that the downhill region of the $P_{pv} - V_{pv}$ curve (i.e. $\frac{dP_{pv}}{dV_{pv}} < 0$) has better damping characteristics than the uphill region (i.e. $\frac{dP_{pv}}{dV_{pv}} > 0$). To meet this requirement, an anti-windup zero upper limiter in controller (6) ensures that when MPP operation is modified by $\frac{dP_{pv,i}}{dV_{pv,i}}ref$ then certainly the PV source will operate in the downhill region.

Remark 2: In the case where the load demand is lower than the maximum PV generation then the modified droop control should achieve accurately power sharing among the PV sources and the dc-bus voltage regulation becomes as close as possible to the desired voltage reference. When the load demand is higher than the available PV generation, the dc-bus voltage will decrease and ultimately become less than the reference. The zero upper limiter is then activated and therefore the $\frac{dP_{pv,i}}{dV_{pv,i}}ref$ is stabilized at zero. In this case, the PV sources operate at MPP while the dc microgrid operates with a reduced dc-bus voltage.

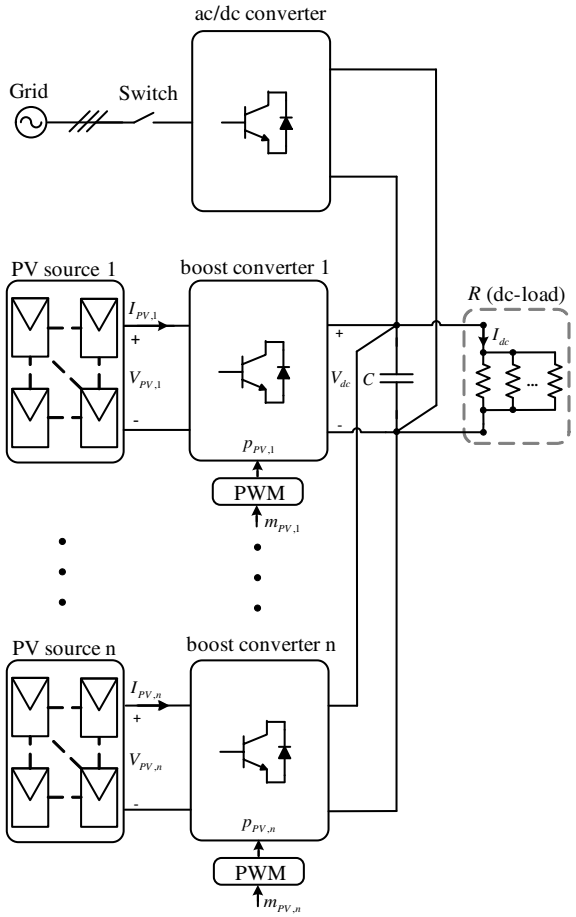

Fig. 2. PV-based dc microgrid.

IV. Stability Analysis

A. Stability Analysis of the Closed-Loop System with the Inner-Loop Controllers

An extensive stability analysis for the closed-loop system with the inner-loop controllers which achieves to prove asymptotic stability can be found in [22].

B. Stability Analysis of the Closed-Loop System with the dP/dV Controller

In the previous subsection, asymptotic stability for the system with the inner-loop controllers was established. Now, making use of the time-scale separation assumption we suppose that the inner-loop controllers converge the currents $I_{pv,i}$ to their reference values $I_{pvref,i}$ very fast, i.e. $I_{pv,i} = I_{pvref,i}$. Using this assumption and incorporating the dP/dV controller (6) we obtain the following closed-loop system

$$I_{pv,i} = -k_{Pmpp,i}\left(\frac{dP_{pv,i}}{dV_{pv,i}} - \frac{dP_{pv,i}}{dV_{pv,i}}ref\right) - k_{Impp,i}z_i \quad (8)$$

$$\dot{z}_i = \frac{dP_{pv,i}}{dV_{pv,i}} - \frac{dP_{pv,i}}{dV_{pv,i}}ref. \quad (9)$$

From steady-state analysis of equations (8)-(9) one can easily arrive at the following equilibrium

$$z_i^* = -\frac{I_{pv,i}^*}{k_{Impp,i}}. \quad (10)$$

Then, after some simple manipulation one can determine the following error dynamics for system (8)-(9)

$$k_{Impp,i}\tilde{z_i} = -k_{Pmpp,i}\frac{d\tilde{P_{pv,i}}}{dV_{pv,i}} - \widetilde{I}_{pv,i} \tag{11}$$

$$\dot{\tilde{z}}_i = \frac{d\tilde{P_{pv,i}}}{dV_{pv,i}} \tag{12}$$

where we defined the error signals as $\tilde{z_i} = z_i - z_i^*$, $\widetilde{I}_{pv,i} = I_{pv,i} - I_{pv,i}^*$ and $\frac{d\tilde{P_{pv,i}}}{dV_{pv,i}} = \frac{dP_{pv,i}}{dV_{pv,i}} - \frac{dP_{pv,i}}{dV_{pv,i}}ref$.

Let us introduce for system (11)-(12) the following Lyapunov function

$$V = \frac{1}{2}k_{Impp,i}\tilde{z_i}^2. \tag{13}$$

Using equations (11)-(12) the time derivative of V can be found

$$\dot{V} = -\widetilde{I}_{pv.i}\frac{d\tilde{P_{pv,i}}}{dV_{pv,i}} - k_{Pmpp,i}\left(\frac{d\tilde{P_{pv,i}}}{dV_{pv,i}}\right)^2. \tag{14}$$

From the $I_{pv} - V_{pv}$ and $\frac{dP_{pv}}{dV_{pv}} - V_{pv}$ characteristics (Fig. 1) it can be easily concluded that the the first term of (14) is negative definite (obviously and the second term) and therefore $\dot{V}$ is negative definite. Hence, the origin is stable and $\lim_{t\to\infty}\tilde{z_i} = 0$.

C. Stability Analysis of the Closed-Loop System with the Droop Controller

Firstly, we examine the existence of an equilibrium point. If we neglect the power losses in the boost converters, then, in steady-state operation the following expression must hold true

$$\sum_{i=1}^{n} P_{pv,i} = P_L \tag{15}$$

where P_L represents the power consumption of the dc load.

Since it is ensured that the PV source will operate in the downhill region, the equation $P_{pv,i} = f_{1,i}\left(\frac{dP_{pv,i}}{dV_{pv,i}}\right)$ can be approximately described by the following linear mathematical relation

$$P_{pv,i} = -\frac{P_{mpp,i}}{y_i}\frac{dP_{pv,i}}{dV_{pv,i}} + P_{mpp,i} \tag{16}$$

where we have defined $y_i = \frac{dP_{pv,i}}{dV_{pv,i}}\mid_{V_{pv,i}=V_{oc,i}}$ with $V_{oc,i}$ the open circuit voltage of the $i-$ PV source and $P_{mpp,i}$ is the MPP power of the $i-$ PV source. Now, substituting (16) into (15) one arrives at

$$\sum_{i=1}^{n}\left(-\frac{P_{mpp,i}}{y_i}\frac{dP_{pv,i}}{dV_{pv,i}} + P_{mpp,i}\right) = P_L. \tag{17}$$

In order to proceed with the analysis we make use of the time-scale separation assumption again, and therefore, we suppose that the middle-loop controllers converge the power-voltage gradients $\frac{dP_{pv,i}}{dV_{pv,i}}$ to their reference values $\frac{dP_{pv,i}}{dV_{pv,i}}ref$ very fast, i.e. $\frac{dP_{pv,i}}{dV_{pv,i}} = \frac{dP_{pv,i}}{dV_{pv,i}}ref$. Taking this into account, we apply expression (7) into (17) and set $P_L = \frac{V_{dc}^2}{R}$, thus we arrive at

$$\sum_{i=1}^{n}\left(-\frac{P_{mpp,i}}{y_i}m_i\left(V_{dc,ref}^2 - V_{dc}^2\right) + P_{mpp,i}\right) = \frac{V_{dc}^2}{R}. \tag{18}$$

Therefore we can conclude that there exists the following unique equilibrium point

$$V_{dc}^* = \sqrt{\frac{\sum_{i=1}^{n}\left(-\frac{P_{mpp,i}}{y_i}m_i V_{dc,ref}^2 + P_{mpp,i}\right)}{\frac{1}{R} + \sum_{i=1}^{n} -\frac{P_{mpp,i}}{y_i}m_i}} \tag{19}$$

where only the positive value has been considered, since the negative value has no physical meaning.

Finally, we determine after some manipulation the following closed-loop error dynamics for equation (3) with the modified droop controller (7) and with respect to the equilibrium point (19)

$$\frac{d\tilde{V}_{dc}^2}{dt} = \frac{2}{C}\left(-\frac{1}{R} + \sum_{i=1}^{n}\left(\frac{P_{mpp,i}}{y_i}m_i\right)\right)\tilde{V}_{dc}^2 \tag{20}$$

where we defined $\tilde{V}_{dc}^2 = V_{dc}^2 - \left(V_{dc}^*\right)^2$. Taking into account that $y_i < 0$, then from equation (20) it is directly concluded that the equilibrium point V_{dc}^* is asymptotically stable. However, this indicates additionally that there will be a small steady-state dc voltage error since $V_{dc}^* \neq V_{dc,ref}$.

V. Tuning the Controllers Gains

A. Tuning the Inner-Loop Controllers Gains

Based on [22], choosing the controller gains as follows with τ_i an arbitrary time constant

$$k_{P,i} = \frac{L_i}{\tau_i} \text{ and } k_{I,i} = \frac{r_i}{\tau_i} \tag{21}$$

the closed-loop response of the $I_{pv,i}$ current is given by a first-order transfer function whose time constant τ_i is a design parameter.

B. Tuning the dP/dV Controller Gains

Since as it is mentioned before the PV source operates in the downhill region, firstly, we approach the equation $\frac{dP_{pv,i}}{dV_{pv,i}} = f_{2,i}\left(I_{pv,i}\right)$ with the following linear mathematical relation

$$\frac{dP_{pv,i}}{dV_{pv,i}} = a_i I_{pv,i} + y_i \tag{22}$$

where we have set $a_i = -\frac{y_i}{I_{mpp,i}}$ with $I_{mpp,i}$ to be the current of the $i-$ PV source at the MPP.

Substituting (8) into (22) one arrives at

$$\frac{dP_{pv,i}}{dV_{pv,i}} = \frac{a_i}{(1 + a_i k_{Pmpp,i})}\left(\frac{1}{a_i}y_i + k_{Pmpp,i}\frac{dP_{pv,i}}{dV_{pv,i}}ref - k_{Impp,i}z_i\right). \tag{23}$$

TABLE I

SYSTEM PARAMETERS

Symbol	*Definition*	*Value*
r_i	Input parasitic resistance of the $i-$boost converter	$0.02\ Ohm$
C	Capacitance of the dc-bus	$1\ mF$
L_i	Inductance of the $i-$boost converter	$2\ mH$
R	Resistance of the dc-load	$300\ Ohm$

Then, using equations (9) and (23) one can obtain

$$\dot{z}_i = -\frac{a_i k_{Impp,i}}{(1+a_i k_{Pmpp,i})} z_i + \frac{1}{(1+a_i k_{Pmpp,i})} y_i + \left(\frac{a_i k_{Pmpp,i}}{(1+a_i k_{Pmpp,i})} - 1 \right) \frac{dP_{pv,i}}{dV_{pv,i}} ref. \quad (24)$$

Finally, the error-dynamics of expression (24) with respect to z_i^* are given by

$$\dot{\tilde{z}}_i = -\frac{a_i k_{Impp,i}}{(1+a_i k_{Pmpp,i})} \tilde{z}_i. \quad (25)$$

From equation (25) one can select the appropriate values for the gains $k_{Pmpp,i}$, $k_{Impp,i}$ in order to achieve the desired time constant response of the closed-loop system with the middle-loop controllers.

C. Tuning the Droop Controller Gains

The tuning of the outer-loop controllers must satisfy two basics objectives: first the PV sources should accurately share the load in proportion to their power ratings and second the closed-loop system must have a desired time constant response. The second demand can be easily satisfied by properly selecting the gain values m_i based on equation (20). For the first demand the following relations must hold true

$$\frac{P_{pv,1}}{P_{mpp,1}} = .. = \frac{P_{pv,i}}{P_{mpp,i}} = .. = \frac{P_{pv,n}}{P_{mpp,n}}. \quad (26)$$

Taking into account relation (16) one can arrive for equation (26) at

$$-\frac{1}{y_1}\frac{dP_{pv,1}}{dV_{pv,1}} + 1 = .. = -\frac{1}{y_n}\frac{dP_{pv,n}}{dV_{pv,n}} + 1. \quad (27)$$

Now, using expression (7) one finally obtains

$$\frac{m_1}{y_1} = .. = \frac{m_i}{y_i} = .. = \frac{m_n}{y_n}. \quad (28)$$

Thus, the above equality must be satisfied in order to achieve accurate power sharing among the PV sources.

VI. SIMULATION RESULTS

In order to indicate the effectiveness of the proposed control scheme and verify our stability analysis, a dc microgrid (as depicted in Fig. 2) with two PV sources, i.e. $i = 2$, is simulated by using MATLAB-Simulink. The response of the system is evaluated, when step changes occur on the local resistive load R and the irradiance. In particular, at $t = 2\,sec$ the irradiance drops from $1000\,\frac{W}{m^2}$ to $900\,\frac{W}{m^2}$, while at $t = 4\,sec$ returns to $1000\,\frac{W}{m^2}$. Additionally, at $t = 6\,sec$ the resistive load changes from $300\,Ohm$ to $280\,Ohm$, while at $t = 8\,sec$ returns to its initial value. Furthermore, it is assumed that the dc microgrid initially operates in islanded mode. However at $t = 10\,sec$, the dc microgrid is connected with the main grid and therefore the dc-voltage is restored at its reference value, i.e. $V_{dc} = V_{dc,ref}$. The maximum power point under nominal conditions of PV source 1 is $683.5\,W$ and of PV source 2 is $341.75\,W$, while it can be measured that $y_1 = y_2 = -40\,\frac{W}{V}$ and $a_1 = 1.042\,\frac{W}{VA}$ and $a_2 = 2.083\,\frac{W}{VA}$. The other system parameters are given in Table I.

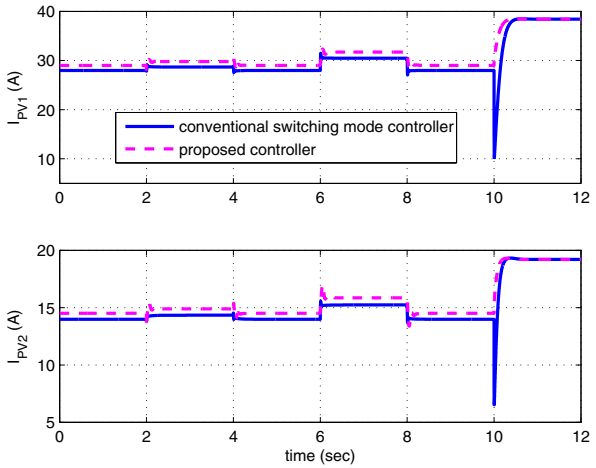

Fig. 3. Response of the currents $I_{pv,1}$ and $I_{pv,2}$.

In order to properly tune the proposed control scheme, we use expressions (20), (21), (25) and (28). Therefore, by setting the controller gains to $k_{P,1} = k_{P,2} = 1$, $k_{I,1} = k_{I,2} = 10$, $k_{Pmpp,1} = 0.14$, $k_{Pmpp,2} = 0.07$, $k_{Impp,1} = 12$, $k_{Impp,2} = 6$ and $m_1 = m_2 = 0.01$ the inner-loop time constant is calculated to be $\tau_i = 0.002\,sec$, while the middle- and outer-loop time constant equal $\tau_m = 0.092\,sec$ and $\tau_{out} \simeq 0.1\,sec$ respectively. Thus, the time-scale assumption holds true and a fast system response can be achieved.

In Fig. 3-5 the response of the system is shown. One can observe that the PV currents and output powers exhibit a satisfactory transient performance and are stabilized very fast to the admissible equilibrium point, while the PV sources accurately share the load in proportion to their power ratings. Finally, as Fig. 5 indicates, the dc voltage is stabilized very close to its reference value with the steady-state error as expected from the theoretical analysis. Furthermore, at $t = 10\,sec$, when the dc microgrid is connected to the main grid, the proposed control scheme drives both PV sources successfully to MPP operation in a smooth, autonomous and seamless manner.

Finally, the proposed control strategy is additionally compared with the conventional switching mode controller. The latter control scheme consists of two separate controllers, namely a MPP and a droop controller. Depending if a MPP or power sharing operation is desired, the proper controller is activated through a switch. From Fig. 3-5 we can observe that until time instant $t = 10\,sec$ the conventional switching mode controller exhibits a similar behavior with the proposed one. However, at $t = 10\,sec$, when the switch is activated and the transition from the droop controller to the MPP algorithm occurs, the system with the conventional switching mode controller displays a stronger transient. This is explained due

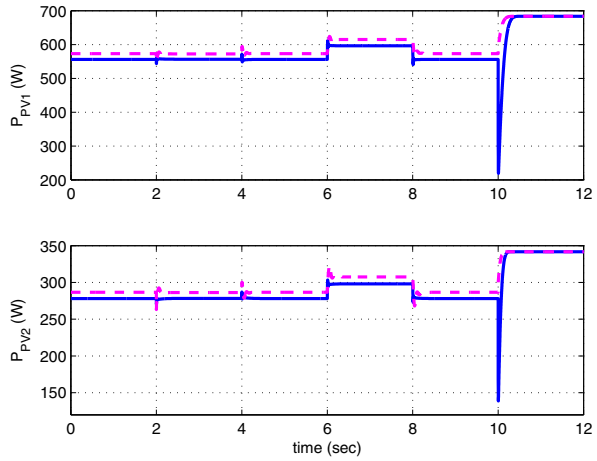

Fig. 4. Response of the PV power outputs $P_{pv,1}$ and $P_{pv,2}$.

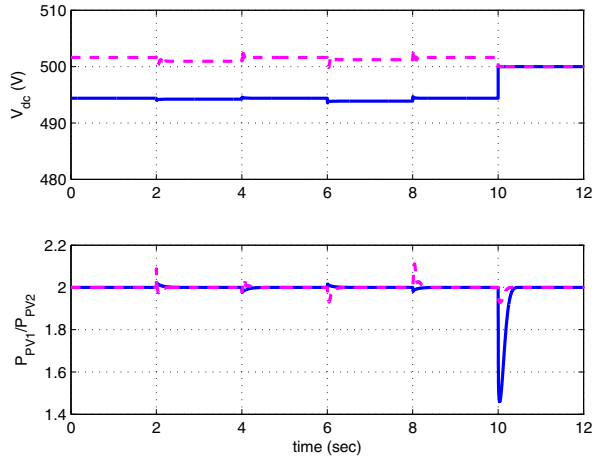

Fig. 5. Response of the dc-bus voltage V_{dc} and the ratio $P_{pv,1}/P_{pv,2}$.

to the fact that when the MPP controller is integrated in the system, its initial conditions are not appropriate, therefore a deep sag on the produced PV power is caused.

VII. Conclusion

In this paper, a unified control design for PV-based dc microgrids is proposed that achieves transition between MPP and droop control operation in an autonomous and seamless manner. Taking into account the accurate models of the PV sources and the power converters, a detailed analysis is deployed that proves stability and convergence to the desired operating point. The effectiveness of the proposed control scheme is further evaluated through simulation results and comparison with the conventional switching mode controller.

References

[1] D. Kumar, F. Zare, and A. Ghosh, "Dc microgrid technology: System architectures, ac grid interfaces, grounding schemes, power quality, communication networks, applications, and standardizations aspects," *IEEE Access*, vol. 5, pp. 12 230–12 256, 2017.

[2] T. Dragicevic, X. Lu, J. C. Vasquez, and J. M. Guerrero, "Dc microgrids-part ii: A review of power architectures, applications, and standardization issues," *IEEE Transactions on Power Electronics*, vol. 31, no. 5, pp. 3528–3549, May 2016.

[3] A. Iovine, S. B. Siad, G. Damm, E. D. Santis, and M. D. D. Benedetto, "Nonlinear control of a dc microgrid for the integration of photovoltaic panels," *IEEE Trans. on Aut. Sci. and Eng.*, vol. 14, no. 2, pp. 524–535, Apr. 2017.

[4] X. Lu, J. M. Guerrero, K. Sun, and J. C. Vasquez, "An improved droop control method for dc microgrids based on low bandwidth communication with dc bus voltage restoration and enhanced current sharing accuracy," *IEEE Transactions on Power Electronics*, vol. 29, no. 4, pp. 1800–1812, Apr. 2014.

[5] K. F. Krommydas and A. T. Alexandridis, "Modular control design and stability analysis of isolated pv-source/battery-storage distributed generation systems," *IEEE Journal on Emerging and Selected Topics in Circuits and Systems*, vol. 5, no. 3, pp. 372–382, Sept. 2015.

[6] L. Mackay, T. Hailu, L. Ramirez-Elizondo, and P. Bauer, "Decentralized current limiting in meshed dc distribution grids," in *Proc. IEEE Int. Conference on DC Microgrids (ICDCM)*, Jun. 2015, pp. 234–238.

[7] N. H. van der Blij, L. M. Ramirez-Elizondo, M. Spaan, and P. Bauer, "A state-space approach to modelling dc distribution systems," *IEEE Trans. on Power Systems*, 2017, to be published.

[8] F. Gao, S. Bozhko, A. Costabeber, C. Patel, P. Wheeler, C. I. Hill, and G. Asher, "Comparative stability analysis of droop control approaches in voltage-source-converter-based dc microgrids," *IEEE Transactions on Power Electronics*, vol. 32, no. 3, pp. 2395–2415, Mar. 2017.

[9] X. Chang, Y. Li, X. Li, and X. Chen, "An active damping method based on a supercapacitor energy storage system to overcome the destabilizing effect of instantaneous constant power loads in dc microgrids," *IEEE Trans. on Energy Conv.*, vol. 32, no. 1, pp. 36–47, Mar. 2017.

[10] L. Herrera, W. Zhang, and J. Wang, "Stability analysis and controller design of dc microgrids with constant power loads," *IEEE Transactions on Smart Grid*, vol. 8, no. 2, pp. 881–888, Mar. 2017.

[11] S. Moayedi and A. Davoudi, "Unifying distributed dynamic optimization and control of islanded dc microgrids," *IEEE Transactions on Power Electronics*, vol. 32, no. 3, pp. 2329–2346, Mar. 2017.

[12] D. I. Makrygiorgou and A. T. Alexandridis, "Stability analysis of dc distribution systems with droop-based charge sharing on energy storage devices," *Energies*, vol. 10, no. 4, Mar. 2017.

[13] Z. Wang, F. Liu, Y. Chen, S. H. Low, and S. Mei, "Unified distributed control of stand-alone dc microgrids," *IEEE Transactions on Smart Grid*, 2017, to be published.

[14] L. Meng, Q. Shafiee, G. F. Trecate, H. Karimi, D. Fulwani, X. Lu, and J. M. Guerrero, "Review on control of dc microgrids and multiple microgrid clusters," *IEEE Journal of Emerging and Selected Topics in Power Electronics*, vol. 5, no. 3, pp. 928–948, Sept. 2017.

[15] R. B. Godoy, D. B. Bizarro, E. T. de Andrade, J. de Oliveira Soares, P. E. M. J. Ribeiro, L. A. Carniato, M. L. M. Kimpara, J. O. P. Pinto, K. Al-Haddad, and C. A. Canesin, "Procedure to match the dynamic response of mppt and droop-controlled microinverters," *IEEE Trans. on Industry Applications*, vol. 53, no. 3, pp. 2358–2368, May 2017.

[16] A. M. Egwebe, M. Fazeli, P. Igic, and P. M. Holland, "Implementation and stability study of dynamic droop in islanded microgrids," *IEEE Trans.on Energy Conversion*, vol. 31, no. 3, pp. 821–832, Sept. 2016.

[17] A. Khorsandi, M. Ashourloo, and H. Mokhtari, "A decentralized control method for a low-voltage dc microgrid," *IEEE Transactions on Energy Conversion*, vol. 29, no. 4, pp. 793–801, Dec. 2014.

[18] A. Elrayyah, Y. Sozer, and M. E. Elbuluk, "Modeling and control design of microgrid-connected pv-based sources," *IEEE Journal of Emerging and Selected Topics in Power Electronics*, vol. 2, no. 4, pp. 907–919, Dec. 2014.

[19] H. Cai, J. Xiang, M. Z. Q. Chen, and W. Wei, "A decentralized control strategy for photovoltaic sources to unify MPPT and DC-bus voltage regulation," in *Proc 2017 American Control Conference (ACC)*, May 2017, pp. 2066–2071.

[20] Y. Mahmoud, W. Xiao, and H. H. Zeineldin, "A simple approach to modeling and simulation of photovoltaic modules," *IEEE Transactions on Sustainable Energy*, vol. 3, no. 1, pp. 185–186, Jan. 2012.

[21] K. F. Krommydas and A. T. Alexandridis, "Nonlinear stability analysis for ac/dc voltage source converters driven by pi current-mode controllers," in *Proc. Eur. Contr. Conf.*, Jun. 2014, pp. 2774–2779.

[22] ——, "Nonlinear design and stability analysis with experimental validation of cascaded pi controlled dc/dc boost converters," in *Proc. 2015 54th IEEE Conf. on Dec. and Contr.*, Dec. 2015, pp. 5043–5048.

[23] ——, "Power controller design and stability analysis of a photovoltaic system with a dc/dc boost converter," in *Proc. 52nd IEEE Conf. on Dec. and Contr.*, Dec. 2013, pp. 3629–3634.

[24] W. Xiao, W. G. Dunford, P. R. Palmer, and A. Capel, "Regulation of photovoltaic voltage," *IEEE Transactions on Industrial Electronics*, vol. 54, no. 3, pp. 1365–1374, Jun. 2007.